International Journal of Refractory Metals and Hard Materials 129 (2025) 107102

Contents lists available at ScienceDirect

International Journal of Refractory Metals and Hard Materials

journal homepage: www.elsevier.com/locate/IJRMHM

Hardmetals with Ru-containing multi-element binders: Composition, constitution and phase formation

Lena Maria Dorner [a], Raquel De Oro Calderon [a,*], Wolf-Dieter Schubert [a], Ralph Useldinger [b]

[a] Institute of Chemical Technologies and Analytics, TU Wien, Getreidemarkt 9/164-CT, 1060 Vienna, Austria
[b] Ceratizit Luxembourg S. à r. l, 101 Route de Holzem, 8232 Mamer, Luxembourg

ARTICLE INFO

Keywords:
Hardmetals
Alternative binders
Ruthenium
Grain growth
Solubilities

ABSTRACT

In spite of the rather high cost of Ru, CoRu binders are commonly used by the industry for the production of cemented carbides with performance demands at high temperatures. In a recent study it was shown that the solubility of W in Co-binders is considerably increased by the addition of Ru (both at low and at high carbon contents), which can significantly affect aspects such as grain growth inhibition, hardness, corrosion resistance and high temperature strength. The present work has extended the study to further binder chemistries: Co, Ni, CoNi and CoNiCr, which have been evaluated both with and without Ru additions. The results indicate that Ru additions increase the solubility of elements like W and Cr for all binder chemistries, both at low and at high carbon contents. The solubility of W is the lowest in the Cr-containing systems (CoNiCr and CoNiCrRu), however, due to the presence of Cr, the total amount of elements in solution is the highest from all binders. The results clearly demonstrate that the WC growth behaviour is significantly affected by the chemistry of the binder system, i.e. the chemical environment of the growing WC grains, which is strongly linked with the chemical activity of carbon in the system.

1. Introduction

In the last years, a new family of metallic alloys has become very popular within the research community, the so-called High Entropy Alloys (HEAs). In contrast to conventional alloys, which consist of one main element to which other alloying elements are added, HEAs present several main elements [1–6]. Outstanding properties have been attributed to this novel family of metallic materials and it is claimed that their use as binder in hardmetals can provide significantly improved performances [7–9].

However, the concept of HEA or multi-component alloy binders cannot easily transfer to hardmetals, in particular if the aim is to have a metallic binder with all elements in solid solution. Due to the interaction between the metallic binder and the hardphase, it is difficult to obtain two-phase materials in which only the hardphase and the alloyed metallic binder are present. Instead, additional phases tend to precipitate when the solubilities in the metallic binder are exceeded. This is the case, for instance, when elements like Cr -with high carbon affinity- are present [10].

In this paper, additions of Ru are used with the aim of obtaining metallic binders with several elements in solution (multi-component binders). Previous studies have also analysed the effect of Ru additions on the microstructure and properties of WC-based cemented carbides, pointing out the enhanced performance particularly at high temperatures. Additions of Ru are reported to provide a reinforcement of the WC/WC and WC/Co interfaces [11], to have a grain growth inhibiting effect [12–15], to increase solid solution hardening of the binder [12–17] and also to enhance FCC to HCP phase transformations in the binder phase [14,15,18,19].

In a recent publication by Schubert et al. [20] it is described, for WC-Co alloys, how the chemistry of the binder phase is significantly altered by the addition of Ru, with considerably higher amounts of W being dissolved in Ru-containing binders. The higher amount of W dissolved in the binder is relevant for understanding the effects of Ru in the hardmetal properties, because the chemistry of the binder determines aspects as important as the size and morphology of the WC phase in the microstructure, the intrinsic hardness of the binder phase, or the corrosion resistance of the alloy. As it is well known, the properties of a hardmetal can differ considerably even within the so-called 2-phase region (region of the phase diagram in which eta carbides and graphite are avoided). The reason is that the W content dissolved in the binder phase (as well as other alloying elements) can be considerably

* Corresponding author.
E-mail address: raquel.oro.calderon@tuwien.ac.at (R. De Oro Calderon).

https://doi.org/10.1016/j.ijrmhm.2025.107102
Received 24 October 2024; Received in revised form 17 February 2025; Accepted 17 February 2025
Available online 18 February 2025

Table 1
Composition of the different alloys prepared. All cemented carbides contain 20 wt% of metallic binder phase, whose compositions are gathered in the table, as well as the name that is used to refer to the alloy thorough the paper.

Binder Alloy (Name)	Binder composition in wt%	Binder composition in at.%	Nominal C contents (wt%) in the mixes
Co	100 Co	100 Co	4.475, 5.2
CoRu	87.2 Co, **12.8 Ru**	92.1 Co, 7.9 Ru	
Ni	100 Ni	100 Ni	4.3, 4.9
NiRu	87.2 Ni, **12.8 Ru**	92.1 Ni, 7.9 Ru	
CoNi	50 Co, 50 Ni	49.9 Co, 50.1 Ni	4.3, 5.2
CoNiRu	43.6 Co, 43.6 Ni, **12.8 Ru**	46.0 Co, 46.1 Ni, 7.9 Ru	
CoNiCr	44 Co, 44 Ni, **12 Cr**	44 Co, 44 Ni, 13.4 Cr	4.3, 5.2
CoNiCrRu	37.6 Co, 37.6 Ni, **12 Cr**, **12.8 Ru**	39.0 Co, 39.2 Ni, 14.1 Cr, 7.7 Ru	

higher at low carbon contents as compared to high carbon alloys [21].

This paper provides a systematic study of cemented carbides containing WC as hardphase, combined with 20 wt% metallic binders with different chemical composition: Co, Ni, CoNi and CoNiCr. This is intended to be a preliminary study to understand whether the trend to increase solubilities in the binder phase, by adding Ru, is reproducible when changing the binder phase composition, and thus evaluate the potential of Ru for changing the chemical composition of metallic binders with a different chemical nature.

2. Experimental procedure

Thermodynamic calculations were carried out for systems containing WC as hardphase, and 20 wt% of different metallic binder compositions (see Table 1), using the commercially available ThermoCalc database TCFE9. Based on the calculations, different gross carbon contents were selected, depending on the chemical nature of the binder (see nominal carbon contents of the samples prepared in Table 1). The carbon contents presented in Table 1 were selected to obtain- for each different binder system- at least one alloy containing eta carbides, and one alloy presenting graphite. Experimentally, the carbon content was adjusted by adding W powder or graphite to the powder mix. A deagglomerated 3 μm FSSS WC powder was provided by Wolfram Bergbau und Hütten AG (Austria).

Standard powder grades (Co, Ni, Cr_2N, W, Ru) were mixed for 2 h in a Turbula mixer without wax. The mixes were pressed at 200 MPa and sintered for 1 h at either 1450 °C - for Co(Ru) and CoNiCr(Ru) samples - or 1480 °C - for Ni(Ru) and CoNi(Ru) samples. Sintering was carried out in a semi-industrial GCA vacuum sintering furnace using Pt-Pt/Rh thermocouples to measure the temperature during the whole sintering process. The heating rate was 10 °C/min up to 1250 °C and then 3 °C/min up to the maximum temperature. The cooling rate was around 15 °C/min down to 1200 °C. The samples were placed on yttria supports in a graphite box together with WC-Co and WC-Ni dummies to minimize carbon and Co/Ni losses during sintering.

The sintered samples were cut into cross sections, embedded and stress-free polished. Sample cross sections were characterized using a Scanning Electron Microscope (SEM) FEI QUANTA 200 ESEM. Energy-Dispersive X-ray Spectrometry (EDS) was used as a semi-quantitative method to identify differences in chemical composition. Binder composition was analysed in wider binder areas to minimize co-detection of WC. At least 5 different point analysis were made in the center of large binder pools (~15 μm in diameter) located in the core part of the samples to give average value with a scatter below 1 wt%.

X-Ray diffraction (XRD) was used to identify the phases in stress-free polished alloys, as well as for lattice parameter measurements of the fcc cobalt binder using a PANanalytical X'Pert PRO diffractometer (CuKα1 radiation). For the lattice parameter measurements, the WC peaks were used as an internal standard.

The hardness of the different alloys was determined on cross sections of the samples, following the norm ISO 3878. Indentations were made with a hardness tester M4U 025 by Emco (Austria) applying loads of 30 kgf. At least 5 indents were used to calculate an average value with a deviation below 10 HV30.

3. Results

3.1. Thermodynamic calculations

Fig. 1 shows the isopleths of WC-20 wt% binder systems containing different binder phases. The compositions selected for preparing experimental samples are marked with red dashed lines. These compositions were selected to provide materials with either eta carbide or graphite, and thus provide information about the solubility of alloying elements at both sides of the carbon window.

The results obtained after characterization of experimentally produced samples are summarized in Table 2. The observed phases indicated in the table have been identified using a combination of metallographic techniques such as light optical microscopy, chemical etchings, XRD analyses and SEM + EDS examinations. The composition of the phases presented in the table corresponds to that obtained from EDS analyses. XRD experiments were also used to provide a calculation of the lattice parameter of the FCC phase in the different alloys.

The microstructures of all materials prepared in this study are presented in Fig. 2 (low carbon alloys), and Fig. 3 (high carbon alloys).

4. Discussion

4.1. Phase formation

As evidenced in Table 2, all samples studied were lying in the phase fields expected from our calculations of the respective phase diagrams (Fig. 1). Low carbon alloys always exhibited eta-carbides besides WC and binder, whereas all high carbon alloys were saturated with carbon and contained graphite precipitations (see Table 2). Only in the case of low carbon materials with Ni and NiRu binders, Ni_2W_4C eta-carbides were formed in the substoichiometric range, while all other low carbon grades exhibited $(Co,Ni)_3(W,Cr)_3C$ eta-phases. This is in good agreement with previous findings reporting that in Ni systems the eta carbides formed present a W-richer Ni_2W_4C structure [21]. The high carbon WC-Co and WC-CoRu grades show small amounts of HCP-binder structure besides the FCC-binder, indicating a martensitic transformation on cooling. Probably also small amounts are present in the low carbon samples but the intensity of the diffraction peaks is too low to identify them univocally. Recent publications have provided important insights on the influence of Ru in the FCC-HCP structures formed in Co-based binders [22,23]. With the exception of Co and CoRu, all other binder chemistries analysed in this study only contained an FCC metallic binder.

As indicated in Table 2, Cr-containing binders - CoNiCr with and without Ru additions- showed Cr-rich carbides in the microstructure of high carbon variants, but not in the low carbon variants. Exemplary EDS mapping images of CoNiCrRu samples at low and high carbon contents are presented in Fig. 4. CoNiCr binders presented similar characteristics. The bright spots observed in the HC-CoNiCrRu materials, in the Cr-mapping of Fig. 4, contain significantly higher Cr-content. As the amount of such carbides is rather small, they could not be detected in the XRD diffraction patterns. In the case of low carbon alloys, EDS mapping in Fig. 5 suggests that Cr is partly dissolved in the eta carbides, which could also be confirmed with several EDS point analyses in this phase (see eta carbide composition in Table 2 with approximately 3 wt% / 7 at. % Cr). In the low carbon materials Cr is apparently mainly divided between the eta carbides and the FCC binder phase. However, the potential formation of a (Cr, W)C layer on WC grains, stabilized by the surface energy, cannot be ruled out [24–26]. In low carbon alloys containing Ru,

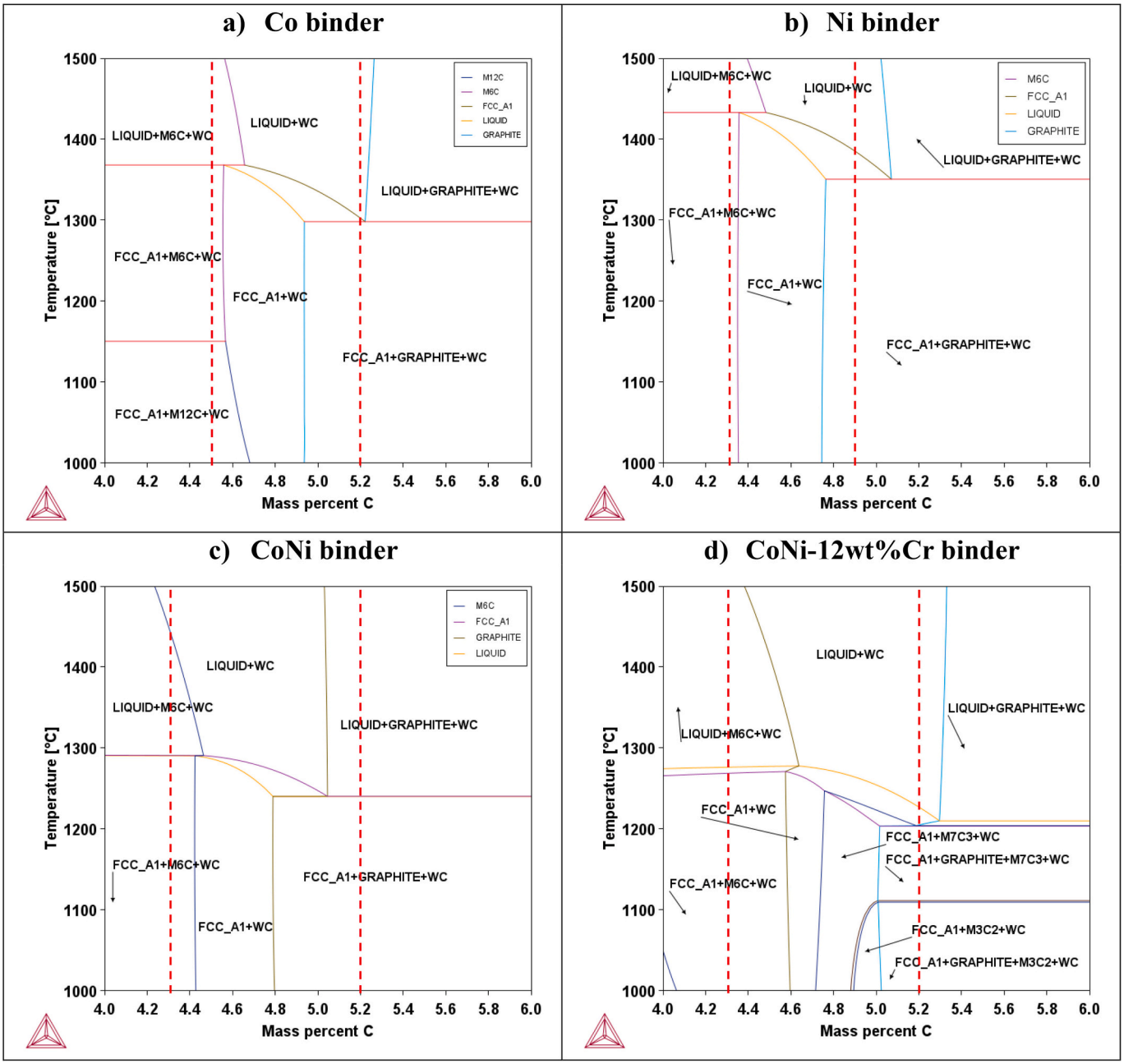

Fig. 1. Isopleths T vs wt% C of different WC-20 wt% binder systems. Calculations were made with the software ThermoCalc using the database TCFE 9. Vertical red dashed lines represent the carbon contents that were prepared experimentally. In the Cr-containing alloy the HCP phase ($(Cr,W)_2C$) has been rejected in the calculation. In the experiments, a carbon loss of approximately 0.05 wt% has to be expected during sintering. (For interpretation of the references to colour in this figure legend, the reader is referred to the web version of this article.)

Table 2
Characteristics of all of the alloys produced in this study.

Alloy	C* (wt%)	Observed phases	Composition of selected phases**		HV30	FCC-lat. par. [Å]
WC-Co	4.475	WC, fcc, eta	Binder	20 W – 80Co (wt%) 7 W – 93 Co (at.%)	917	3.577
			η (Co_3W_3C)	75 W - 25Co (wt%) 49 W – 51Co (at.%)		
	5.2	WC, fcc, hcp, graphite	Binder	4 W – 96Co (wt%) 1 W – 99Co (at.%)	808	3.552
WC-CoRu	4.475	WC, fcc, eta	Binder	26 W – 8Ru – 66Co (wt%) 11 W – 6Ru – 83Co (at.%)	1034	3.610
			η (Co_3W_3C)	76 W – 1Ru - 23Co (wt%) 49 W – 2Ru – 49 Co (at.%)		
	5.2	WC, fcc, hcp, graphite	Binder	6 W – 10Ru – 84Co (wt%) 2 W – 6Ru – 92Co (at.%)	923	3.581
WC-Ni	4.3	WC, fcc, eta	Binder	28 W – 72Co (wt%) 11 W – 89Ni (at.%)	775	3.582
			η (Ni_2W_4C)	80 W – 20Ni (wt%) 58 W – 42Ni (at.%)		
	4.9	WC, fcc, graphite	Binder	8 W – 92Ni (wt%) 3 W – 97 Ni (at.%)	769	3.545
WC-NiRu	4.3	WC, fcc, eta	Binder	34 W – 7Ru – 59Ni (wt%) 15 W – 5Ru – 80Ni (at.%)	831	3.617
			η (Ni_2W_4C)	79 W – 1.5Ru – 19.5Ni (wt%) 43 W – 2Ru – 55Ni (at.%)		
	4.9	WC, fcc, graphite	Binder	11 W – 9Ru – 80Ni (wt%) 4 W – 6Ru – 90Ni (at.%)	813	3.577
WC-CoNi	4.3	WC, fcc, eta	Binder:	25 W – 32Co – 43Ni (wt%) 10 W – 38Co – 52Ni (at.%)	856	3.581
			η (M_6C)	79 W – 11Co – 10Ni (wt%) 54 W – 24Co – 22Ni (at.%)		
	5.2	WC, fcc, graphite	Binder	5 W – 34Co – 61Ni (wt%) 2 W – 35Co – 63Ni (at.%)	764	3.547
WC-CoNiRu	4.3	WC, fcc, eta	Binder	30 W – 7Ru – 25Co – 38Ni (wt%) 12 W – 5Ru – 33Co – 50Ni (at.%)	903	3.613
			η (M_6C)	79 W – 1Ru – 10Co - 10Ni (wt%) 53 W – 1Ru – 23Co – 23Ni (at.%)		
	5.2	WC, fcc, graphite	Binder	9 W – 10Ru – 38Co – 43Ni (wt%) 3 W – 6Ru – 42Co – 49Ni (at.%)	818	3.577
WC-CoNiCr	4.3	WC, fcc, eta	Binder	20 W – 5Cr – 31Co – 44Ni (wt%) 7 W – 6Cr – 35Co – 52Ni (at.%)	989	3.574
			η (M_6C)	75 W – 3Cr – 12Co - 10Ni (wt%) 48 W – 7Cr – 23Co – 22Ni (at.%)		
	5.2	WC, fcc, graphite, Cr-carb	Binder	4 W – 8Cr – 38Co – 50Ni (wt%) 1 W – 9Cr – 39Co – 51Ni (at.%)	832	3.547
WC-CoNiCrRu	4.3	WC, fcc, eta	Binder	24 W – 8Ru – 5Cr – 25Co – 38Ni (wt%) 10 W – 6Ru – 7Cr – 32Co – 45Ni (at.%)	1058	3.610
			η (M_6C)	74 W – 1Ru - 3Cr – 10Co - 12Ni (wt%) 49 W – 1Ru - 7Cr – 21Co – 22Ni (at.%)		
	5.2	WC, fcc, graphite, Cr-carb	Binder	6 W – 10Ru – 9Cr – 31Co – 44Ni (wt%) 2 W – 6Ru – 11Cr – 33Co – 48Ni (at.%)	912	3.583

* Nominal carbon content.
** Note that the Co/Ni ratio (50/50) in the nominal composition of the binder phase is altered in the as-sintered materials to a lower Co/Ni ratio (about 42/58) due to preferred cobalt losses by evaporation. C not considered in EDS analyses.

also small amounts of Ru - 1 wt%/2 at.%- are observed with EDS analysis in the eta carbide, but this might as well be due to secondary X-ray fluorescence from subjacent/intergrown binder.

Further examination of the Cr-rich carbides was carried out by etching away the metallic binder phase -with concentrated HCl- in the CoNiCr high carbon alloys (see Fig. 5a, b). A detail on the microstructure before etching the binder can be observed in Fig. 5c. As it is evidenced in Fig. 5, Cr-rich carbides appear intergrown between the WC grains, as typically observed in Co-based Cr-containing materials with M_7C_3 precipitations [10,27]. Point analyses in these Cr-rich carbides show, as expected, high amounts of Cr, but also a certain amount of Ni and Co. Considering that a deep-etching of the binder was carried out before the analysis, the presence of binder elements (Co and Ni) can be ruled out, which means that these elements are most likely taking part in the carbide. The presence of Co and Ni in the carbide suggests that the carbide presents an M_7C_3 structure, as M_3C_2 typically show high Cr-content and almost negligible amounts of other elements like Co and Ni. This observation is also in line with the thermodynamic calculation presented in Fig. 1 for the CoNiCr system. According to the calculation, on cooling from the sintering temperature, M_7C_3 carbides would precipitate, and only at low temperatures this carbide would be transformed into M_3C_2. It is however unlikely that this transformation would take place at the cooling rates typically obtained on sintering.

4.2. Composition of the binder phase

Metallic binder phases in hardmetals consist always of alloys in which a certain amount of the elements present in the hardphase (W and C) have been dissolved during sintering. The solubility of elements in the metallic binder depends on the chemical nature of the binder phase, as well as on the carbon activity in the system. As previously reported, marked differences in W solubility in 2-phase hardmetals with Ni-based binders (caused by the different carbon contents), provide alloys with remarkable differences in corrosion resistance and binder hardness (due to the differences in the amount of W dissolved) [21].

Fig. 6 shows the W content in the binder phases of all the different alloy families, with and without Ru additions. Carbon (also dissolved in the binder matrix) was not considered in EDS analyses. Low carbon variants are represented on the left, and high carbon variants on the right. The low carbon variants can dissolve significantly higher amounts of W, as compared with the high carbon equivalents. When comparing all variants without Ru, the maximum solubility of W is observed, as expected, in Ni binders, followed by CoNi, Co and CoNiCr binders. The same trend is observed when comparing all Ru-containing samples. This is valid both for low carbon alloys as well as for high carbon alloys.

Both in the low and in the high carbon variants, it is evident that the solubility of W in the binder phase is significantly higher in Ru containing alloys, as compared to the same alloy without Ru-additions.

The degree of alloying in the binder phase (i.e. number of foreign atoms in solution) is better evaluated by representing the concentrations in atomic percent (at. %). The solubility (in at. %) of both Cr and W in CoNi and CoNiCr alloys, with and without Ru, are represented in Fig. 7 (left low carbon alloys and right high carbon alloys). For both Cr and W, the solubility in the metallic binder increased with the addition of Ru.

The differences in Cr-solubility between low and high carbon variants are smaller than the differences in W-dissolved. Furthermore, the solubility of Cr at high carbon contents is higher than that in the low carbon variant, a striking trend that is inversed to that observed for W. A certain increase in the concentration of Cr in the binder phase at increasing carbon contents can be explained by the differences in the volume fraction of metallic binder. Within the two-phase region, as the amount of carbon increases, the volume of metallic binder (FCC) decreases due to the precipitation of WC at higher carbon activities (which is linked to the lower solubility of W in the metallic binder). Thus, the metallic FCC phase becomes more and more concentrated in Cr, until the maximum solubility is reached and Cr-rich carbides precipitate. This phenomena is further described in following sections. Under experimental conditions the amount of Cr-rich carbides formed during cooling might be lower than the amount that would be expected under equilibrium, e.g. due to nucleation problems, which could cause a certain degree of Cr super-saturation in high carbon alloys.

When comparing CoNi and CoNiCr binders in Fig. 7, it is evident that additions of Cr to the binder phase decrease considerably the amount of W in solution (both in the low carbon and in the high carbon variants). Therefore, as shown in Fig. 6, the W solubility is lower for CoNiCr families as compared to all other families studied (both with and without Ru additions). However, in these samples Cr is present as alloying element in the binder phase, and this leads to a higher total amount of elements dissolved in the binder, if considering the solubility of both W and Cr (see Fig. 8). Similar observations have already been reported for Ni-based binders [21]. If taking as a reference a Co-binder, it is clear from these experiments that additions of elements with a lower carbon affinity (like Ni and Ru) tend to increase the solubility of W in the binder phase, while the addition of elements with a high carbon affinity (like Cr) tend to decrease the solubility of W in the binder phase. P.K. Mehrotra and P.B. Trivedi have reported on how alloying elements may affect the carbon range over which no C- porosity or eta phase form [28].

In Fig. 8, the total solubility (in at.%) for the elements W and Cr, is represented for all alloy families. It is clear from this graph that the CoNiCr alloys (with or without Ru) present the higher amount of alloying elements dissolved in the binder phase (if considering W and Cr as the alloying elements). As in all other binders, the total solubility of elements in Cr-containing binders is higher in the low carbon variant and lower in the high carbon, although the difference between low and high carbon is rather small (mainly because of the rather similar Cr solubility in high and low carbon alloys).

4.3. FCC lattice parameter

The lattice parameter of the FCC phase is affected by the amount (and size) of the alloying elements dissolved in the binder. Fig. 9 shows the lattice parameter measured for all different binder phases used in this study, both for the low carbon (LC) and for the high carbon (HC) variants. In general, low carbon variants always present higher FCC lattice parameters than their equivalent high carbon variants, mainly because of the differences in W solubility at low and high carbon contents. Additions of Ru to the binders always result in an increase in the lattice parameters, partly because of the dissolution of Ru, but most importantly because of the higher amounts of W dissolved (W being a larger atom than Ru).

The differences between lattice parameters at low and high carbon alloys are indicated with numbers in Fig. 9. As the amount of W is not expected to vary dramatically for samples that are within the eta carbide or withing the graphite region (at least in the vicinity of the respective carbon limits), the difference in the lattice parameter can be seen as an indirect indication of the size of the carbon window. As expected, this difference is the largest in Ni binder (0.037), followed by the CoNi binder (0.034). CoNiCr and Co binder show very similar values. This might indicate a trend in decreasing the carbon window in the sequence Ni > CoNi>CoNiCr/Co. When considering Ru-additions, the difference in lattice parameters is higher than in the same alloy without Ru, suggesting that the carbon window might be broader in Ru-containing materials.

4.4. WC grain size and morphology

All low carbon alloys (Fig. 2) exhibit a clearly finer WC microstructure than their high carbon counterparts (in Fig. 3). This is the case for all binder compositions, with or without Ru addition. In general, Ru-containing alloys always show even finer microstructures (stronger WC growth inhibition) than the respective Ru-free samples, both in the low carbon and in the high carbon variants.

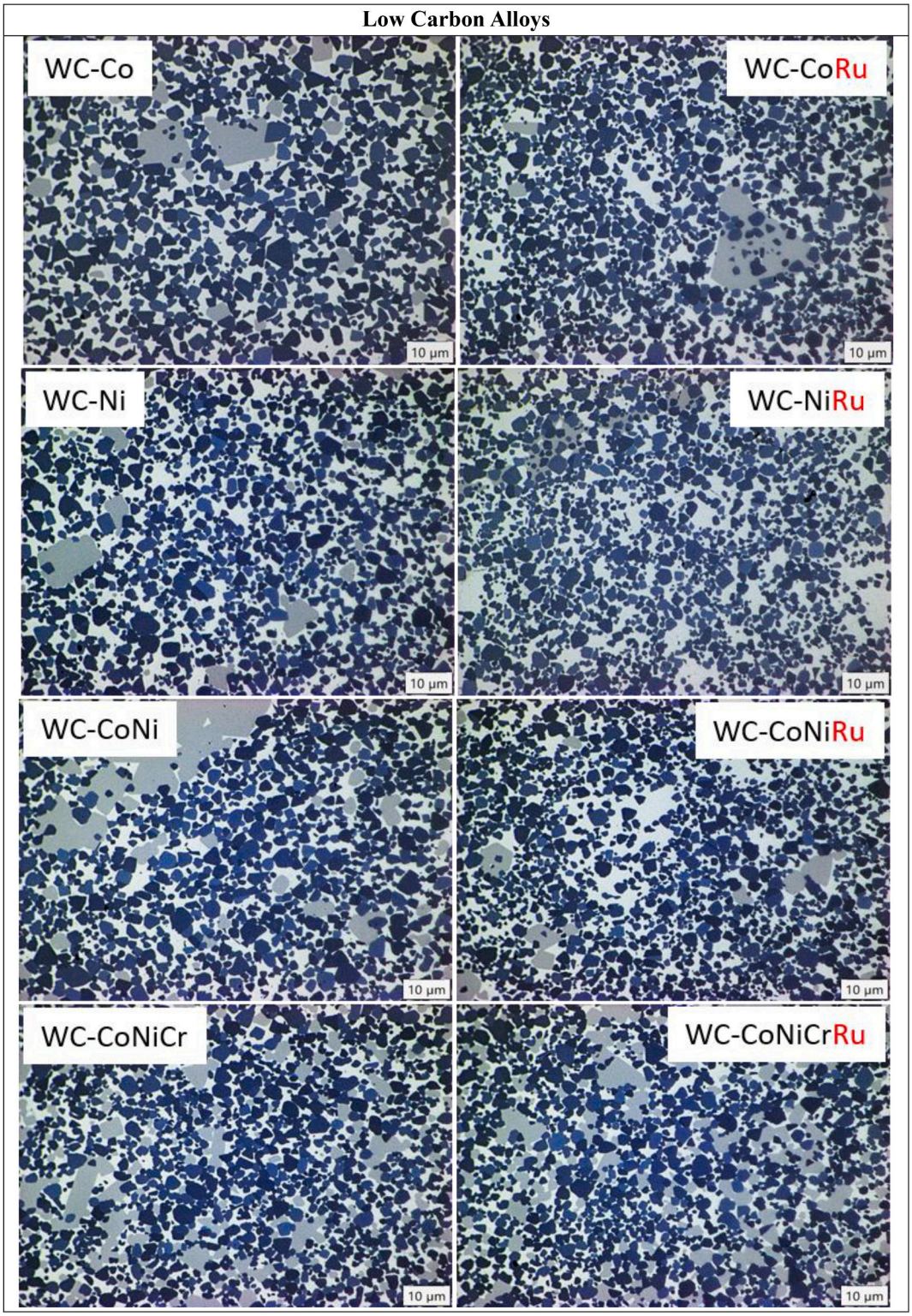

Fig. 2. Microstructure of low carbon alloys, without (left) or with Ru additions (right). White phase is the metallic binder, light grey are eta carbides and dark grey is WC.

The stronger WC growth inhibition in the low carbon variants (presented in Fig. 2) is demonstrated by a significantly higher portion of WC fines and more polygonal WC grains (rounded morphology). In contrast, high carbon alloys (Fig. 4) always demonstrate coarser and more facetted WC grain growth. The most remarkable differences in grain growth are observed on comparing WC-Ni alloys with low and high carbon contents (see Fig. 10).

It is striking that the low carbon WC-Ni and WC-NiRu grades exhibit a finer microstructure than the respective WC-Co and WC-CoRu low carbon variants. Both the significant differences between low and high carbon alloy, and the important grain growth inhibition in Ni-binders with low carbon contents (in equilibrium with eta carbides) have also been previously reported [10,29,30]. Microstructures of the low carbon WC-CoNi and WC-CoNiRu lie in-between those of the low carbon Co and

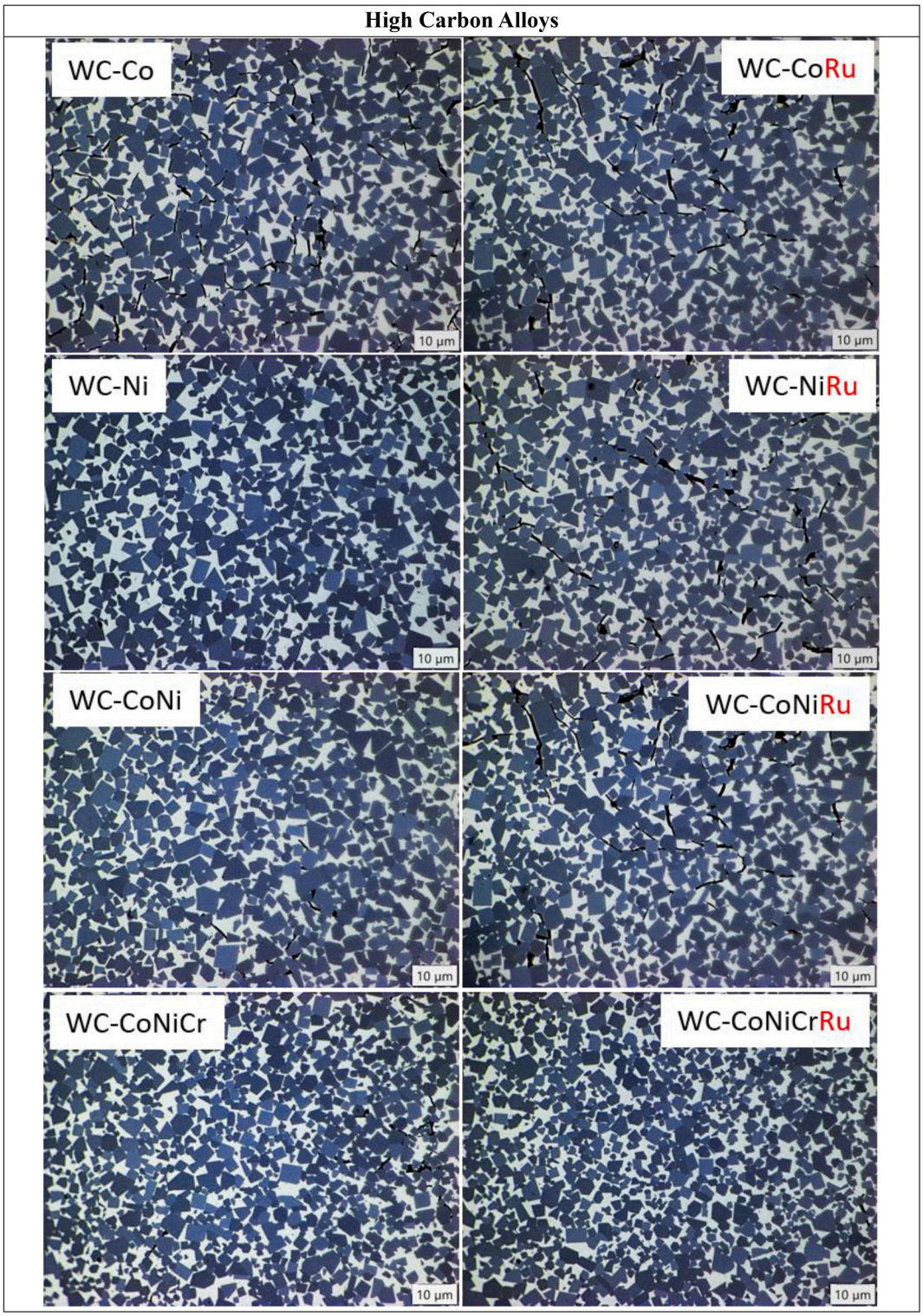

Fig. 3. Microstructure of high carbon alloys, without (left) or with Ru additions (right). White phase is the metallic binder, black regions contain graphite and dark grey is WC.

Ni-based binders.

Additions of Cr lead to a further WC grain refinement in high carbon WC-CoNiCr(Ru) alloys. However, in case of the low carbon variants the WC-CoNiRu microstructure seems even finer than that of the WC-CoNiCrRu grade (see comparison in Fig. 11). Looking at the solubility data in Table 2, the tungsten solubility in CoNiRu-LC is 30 wt%, while in CoNiCrRu-LC it is only 24 wt% (as Cr reduces the W solubility). Additionally, in CoNiCrRu alloys only 5 wt% Cr is present in the LC variant, as compared to the 9 wt% in the HC variant.

In all cases, WC grain growth inhibition is related to a higher W solubility in the alloy binder (see Table 2); it is most pronounced in the WC-NiRu LC grade, followed by WC-CoNiRu LC and WC-Ni LC. Additions of chromium inhibit WC grain growth but at the same time, the addition of Cr to the binder lowers the W solubility (see Table 2) and

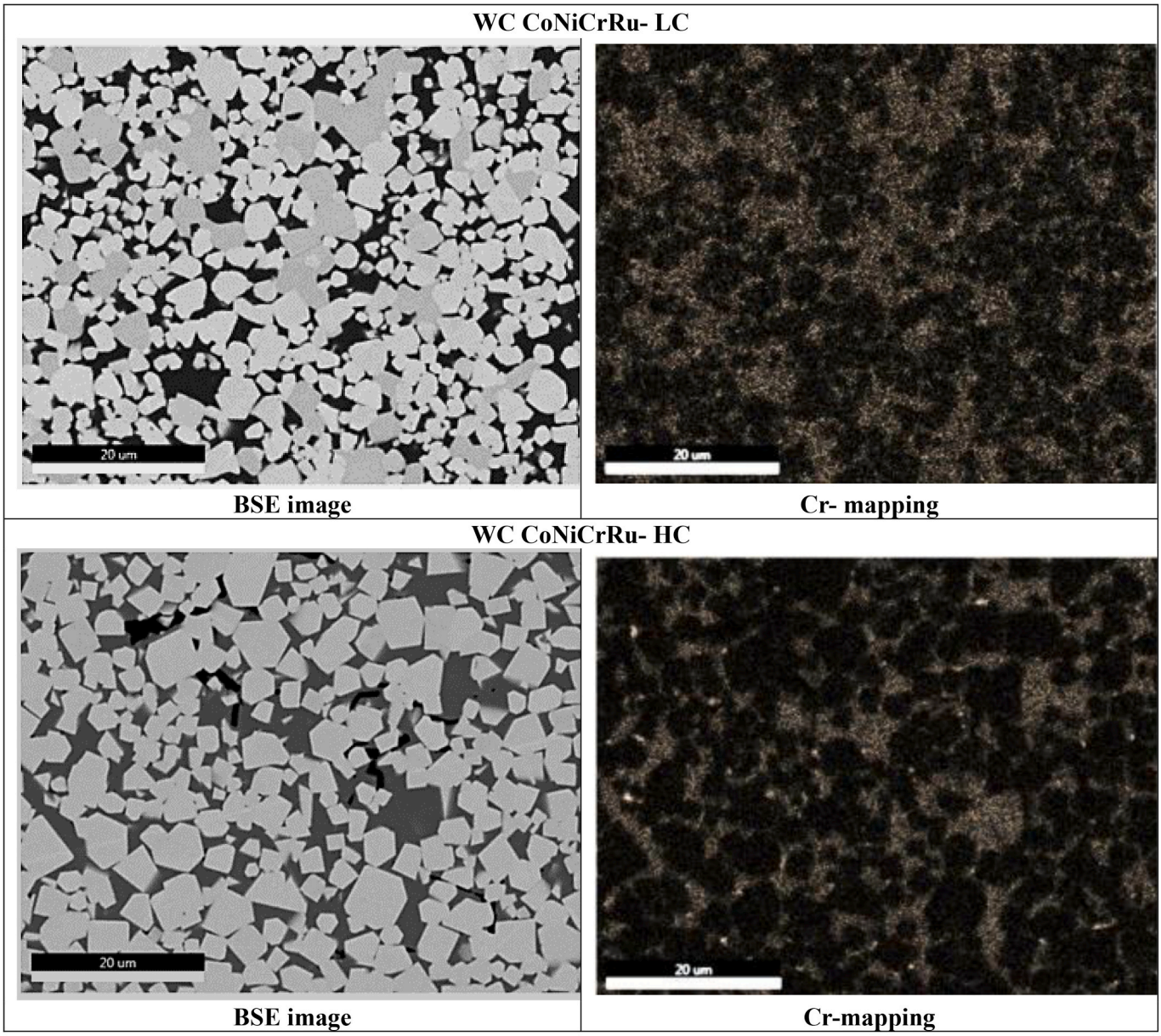

Fig. 4. Image and EDS mapping of the samples WC-20 wt% (CoNiCrRu binder): Above: 4.3 wt%C (containing eta carbides), Below: 5.2 wt%C (containing graphite precipitations). On the left, backscattered electrons images. On the right, Cr-mapping. Bright white areas in the high carbon sample are Cr-rich carbides.

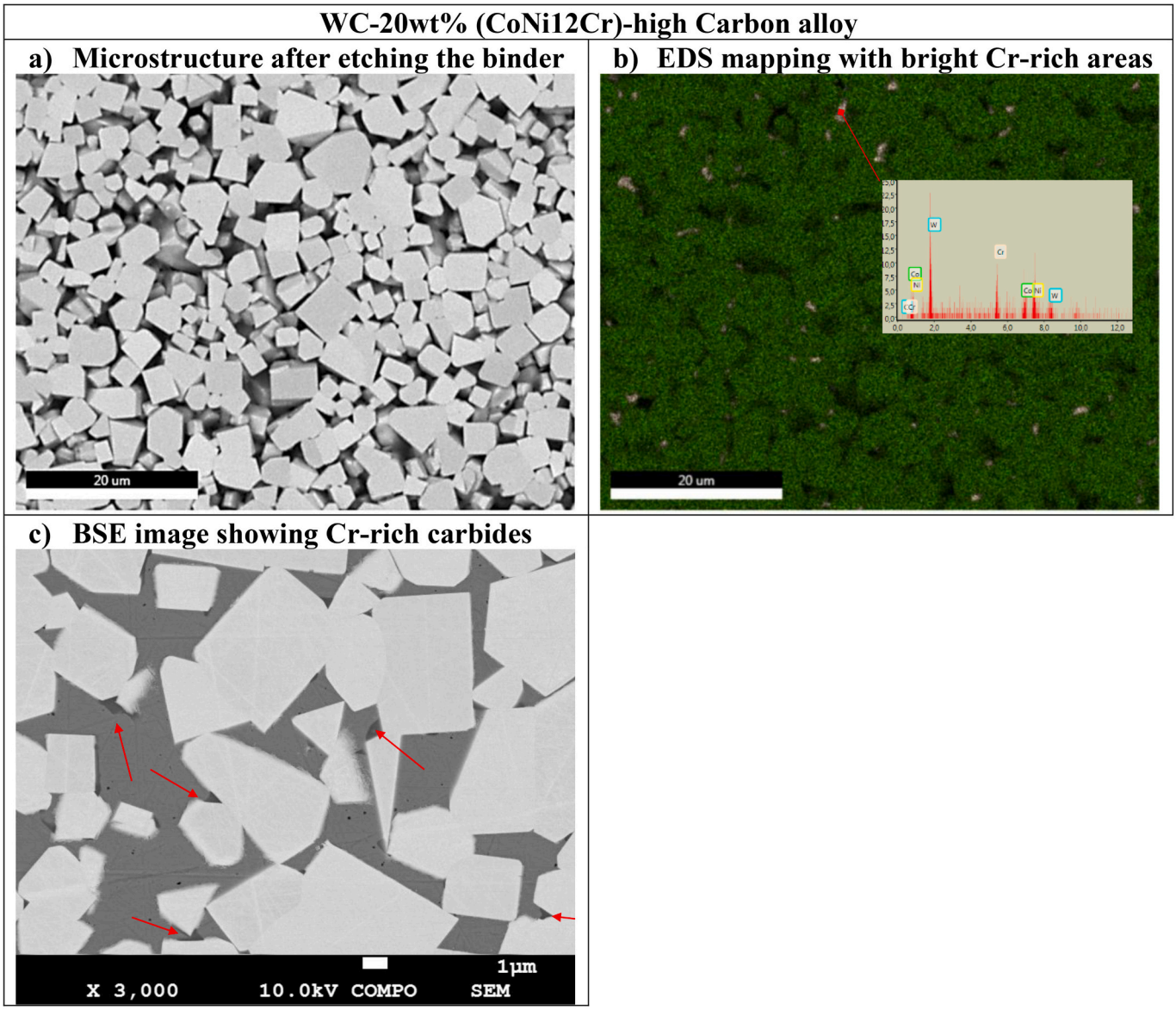

Fig. 5. Image and EDS mapping of the high carbon alloy WC-20 wt% (CoNiCr binder): a) Microstructure after deep-etching during 3 min with concentrated HCl to remove the metallic binder. b) EDS mapping of the etched area shown in a), including the spectra obtained when doing a point analysis on the Cr-rich brigth areas. c) BSE image of an unetched sample showing the morphology and growth behaviour of the Cr-rich carbides (intergrown in the WC phase).

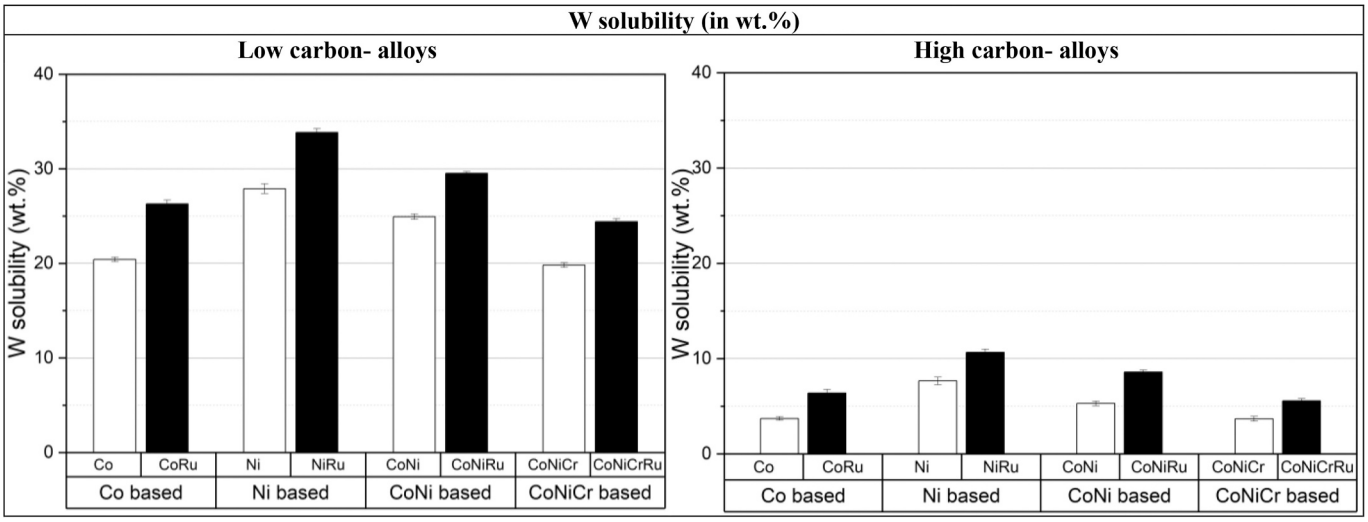

Fig. 6. W solubility in different binder alloys: low carbon alloys (left) and high carbon alloys (right). White bars represent binders without Ru additions (Co, Ni, CoNi, CoNiCr from left to right). Black bars represent binders with Ru additions (CoRu, NiRu, CoNiRu, CoNiCrRu from left to right).

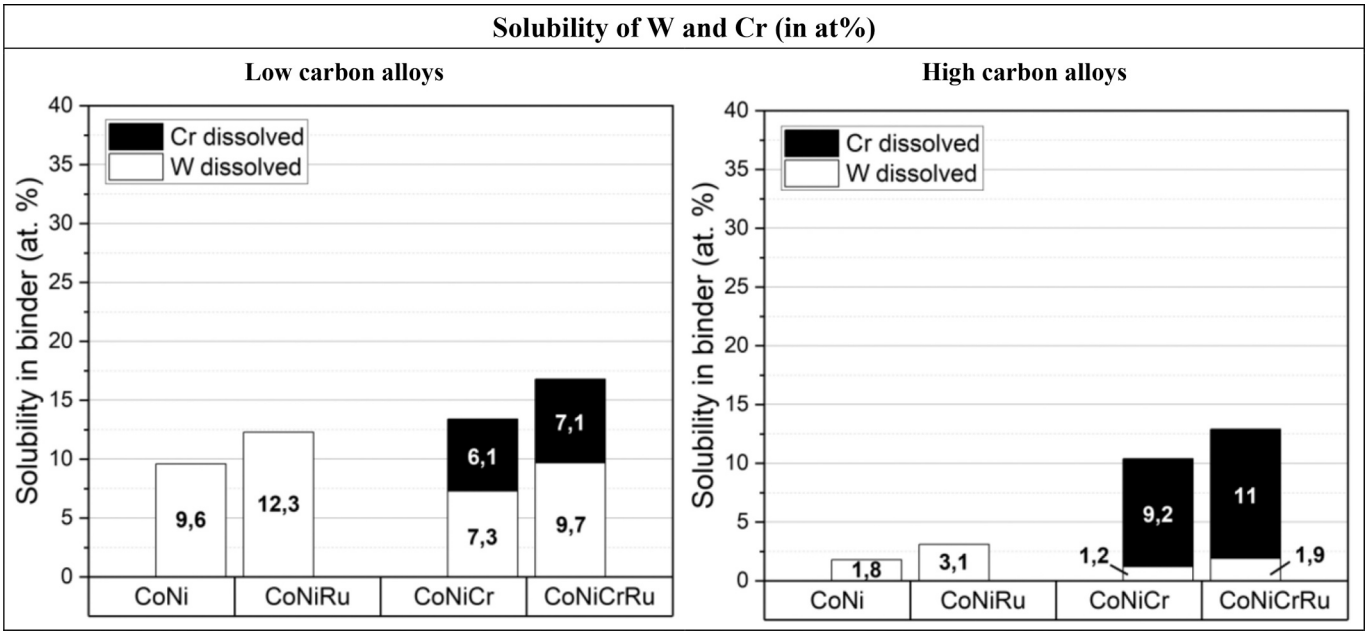

Fig. 7. Solubility of W and Cr in the binder phase, expressed in at. %.

therefore CoNiRu-LC microstructures seem slightly finer than those of CoNiCrRu-LC binder (see Fig. 10), as the latter contains lower W in solution. In contrast, in the high carbon variants the influence of Cr on WC growth inhibition can be well observed (see Fig. 10). High carbon WC-CoNiCrRu samples present finer microstructures than high carbon WC-CoNiRu alloys. In these alloys, for which the W dissolved is significantly lower than in their low carbon counterparts, Cr clearly works as a grain refiner.

4.5. Alloy hardness

Hardness values of the alloys produced in this study are plotted in Fig. 12. The hardness of the individual alloys is determined mainly by both the fineness of the WC microstructure, but also by the individual binder alloy hardness. This has been demonstrated in case of Ni alloys [21].

Hardness of the low carbon variants differ between 1058 HV30 and 775 HV30. In this case also the influence of different amounts of eta-phase must be considered, which makes the comparison more complex. The highest hardness was obtained for WC-CoNiCrRu, but in this case the portion of eta-phase was also the largest. WC-Co and WC-CoRu variants are in general harder than WC-Ni(Ru) or WC-CoNi(Ru) grades. The lower grain size when adding Ru make these differences less pronounced.

In case of the high carbon variants, the hardness differs between 923 HV30 and 764 HV30. As compared to the low carbon variants, it is expected to obtain lower hardness values in high carbon alloys: partly because of the coarser microstructures, but also due to the absence of eta carbides in the microstructure. In the case of the high carbon alloys the hardness values of the composite are more influenced by the individual binder hardness, the only exception being the high hardness of the high carbon WC-CoNiCrRu grade, with a hardness of 912 HV30, due to its significantly finer WC microstructure (see Fig. 4). The hardness is the highest in Co grades, followed by CoNi and Ni-grades, as one might

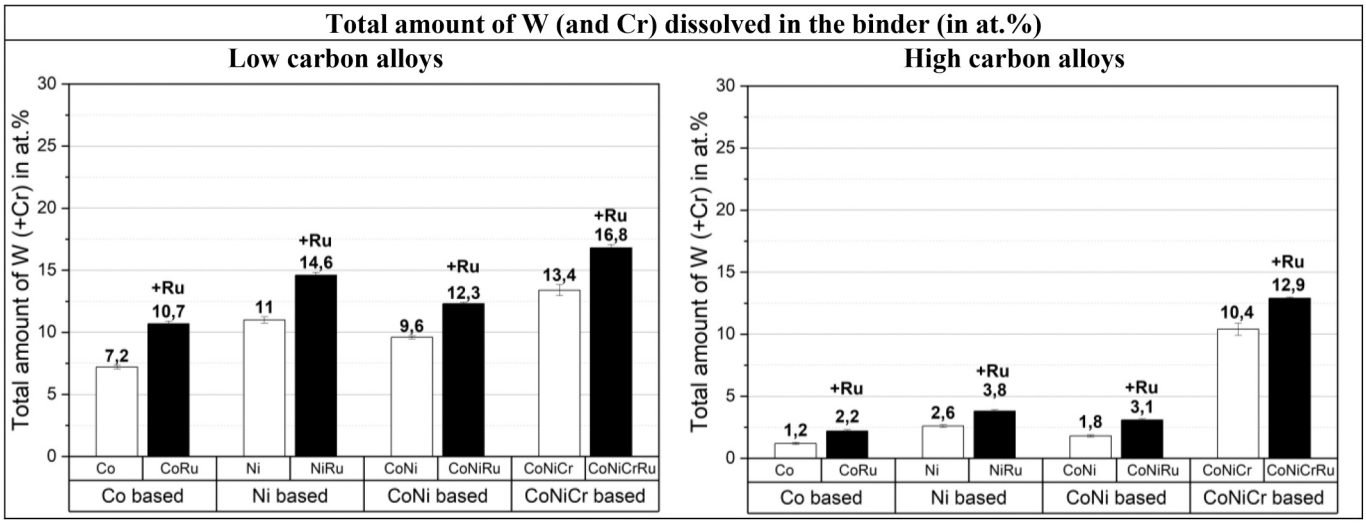

Fig. 8. Total amount of W and Cr dissolved in the binder phase, expressed in at. %.

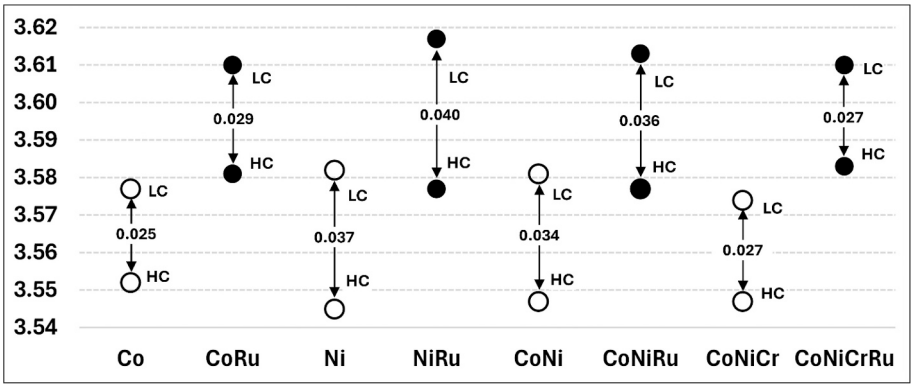

Fig. 9. Graphic representation of the FCC lattice parameters of all samples (individual values are presented Table 2); lower values refer to HC variants, higher values to LC grades. The difference in lattice parameter between LC and HC variants of each alloy system most likely refers to the width of its carbon window. In case of CoNiCr and CoNiCrRu chromium carbide(s) can form within the window. Note that Co and CoRu alloys also exhibit small amounts of HCP-Co.

expect from industrial practice.

4.6. Agreement between theoretical calculations and experimental findings

Thermodynamic calculations have been used to determine the nominal carbon contents needed for obtaining materials with either eta carbides or graphite. As Ru is not assessed in the TCFE9 database, the calculations were only made for alloys without Ru. It is expected that, the presence of Ru, would widen the carbon windows, as already described for Co and CoRu binders by Trivedi & Mehrotra [31]. This is also supported by the experimental studies presented in [20] as well as by the studies presented in this paper, which confirm that the addition of Ru increases the solubility of W in the metallic binders. This, in turn, means that larger sub-stoichiometric compositions are necessary in Ru-containing binders to promote the precipitation of eta carbides.

As shown in the phase diagrams in Fig. 1, in the case of Co, Ni and CoNi alloys, the calculations predict a two-phase region in which only WC and FCC phases are stable. In contrast, in case of the Cr-containing alloys, additional carbides are predicted. M_7C_3 and M_3C_2 carbides are stabilized at the higher carbon contents, while an HCP $(Cr, W)_2C$ carbide is predicted at low carbon contents. As this phase has been rarely observed in praxis, the calculation presented in Fig. 1-d was run rejecting the HCP phase. The diagram from Fig. 1-d (WC-CoNiCr) shows a two-phase region (WC + FCC) which is decreased in size from the high carbon side due to the stabilization of M_7C_3 and M_3C_2 carbides (Cr-rich carbides). The experimental findings are in line with this calculation, as low carbon samples do not show any additional carbides -apart from eta carbides- in the microstructure, but the high carbon samples did.

Further details on the calculation in the WC-CoNiCr system are provided in Fig. 13, which shows the equilibrium for varying carbon contents, for a constant temperature of 1000 °C. This temperature has been selected because it is the temperature at which it is traditionally considered that the binder composition of hardmetals is “frozen-in”, as the diffusion of W is not considered as significant. Fig. 13- a) shows the evolution of stable phases as the amount of C increases, and Fig. 13-b) the evolution in the composition of the FCC phase. These calculations evidence how the W content decreases in the binder phase as the carbon content increases, reaching a maximum and a minimum value at low carbon and high carbon sides of the two-phase region, respectively. The lowest limit – around 4.6 wt% C – provides the maximum W solubility, and the highest limit – around 4.7 wt% C- the lowest solubility of W in the binder. In case of Cr the evolution is slightly different. From the lower side of the carbon window – 4.6 wt% C-, the Cr content in the binder phase increases at increasing the C contents, until the maximum solubility is reached −10.2 wt% Cr- and thus M_7C_3 carbides precipitate. It is obvious by the calculation, that the maximum solubility of Cr is in this case not observed at the lowest carbon contents of the carbon window, but at the carbon content at which the M_7C_3 carbide is stabilized. This trend is different to that of W, the reason being that W takes

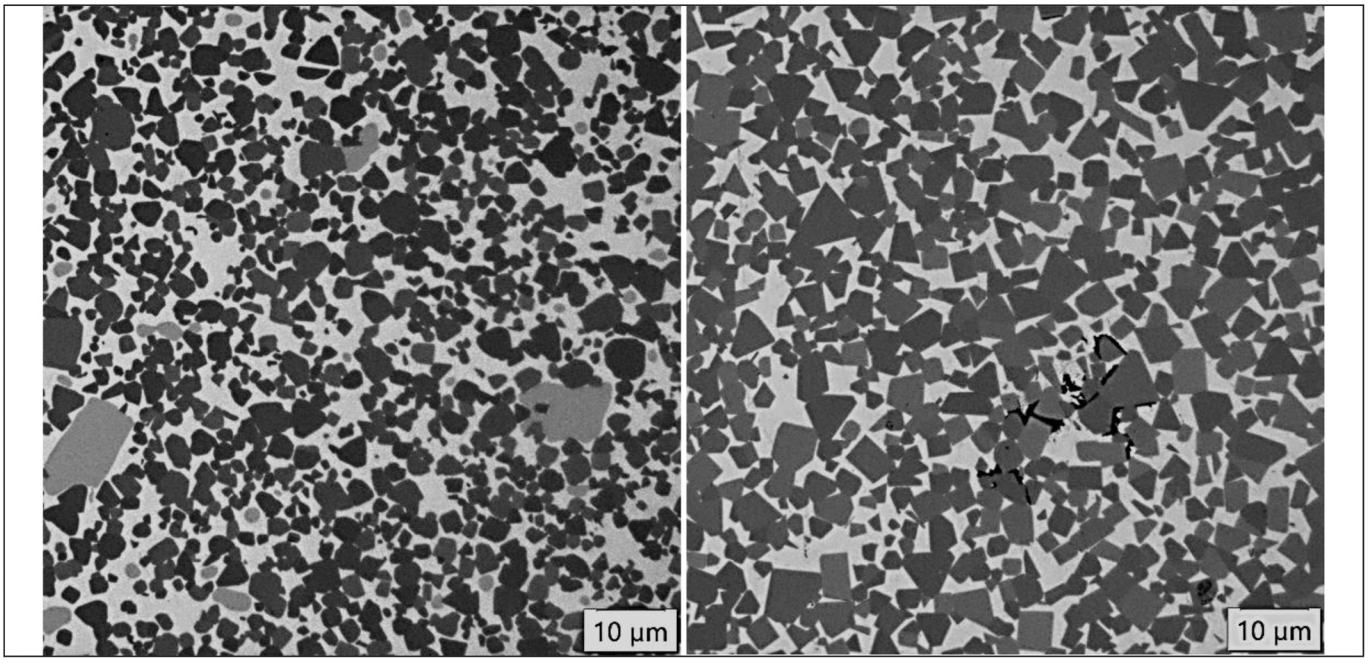

Fig. 10. WC grain growth in LC (left) and HC (right) WC-20 wt% Ni alloys. Note the strong growth inhibition in the LC variant. Further grain refinement occurs on Ru addition as shown if Fig. 2 and Fig. 3.

place in the formation of the hardphase WC. Thus, at increasing C contents higher amounts of WC are formed, and the amount of W in the binder decreases. Cr, however remains dissolved in the binder phase and, because the volume of metallic phase FCC decreases at increasing C contents, the FCC phase becomes more concentrated in Cr, until the solubility limit is reached and M_7C_3 Cr-rich carbide is stabilized.

The predicted trend in solubility of W between low and high carbon alloys is in agreement with the experiments, with a significant decrease in W solubility between low carbon and high carbon alloys. However, in the case of Cr alloys the trends observed experimentally are inverse to those presented in the calculation. According to the calculation, low carbon alloys should dissolve slightly higher Cr contents than high carbon alloys. However, it must be noted that -in praxis- difficulties for the nucleation of the Cr-rich carbides (in this case M_7C_3 and/or M_3C_2) may give rise to binders that are slightly super saturated in Cr at the high carbon region. This might be the reason why thermodynamic calculations and experiments are in slight disagreement.

Fig. 13-c shows the distribution of Cr between the different phases at 1000 °C. It evidences that certain amounts of Cr are expected to be dissolved in the eta carbides, around 0.2 wt%. However, experimental measurements provide considerable higher Cr solubilities in the eta carbide (around 3 wt% Cr/ 7 at.% Cr- see Table 2). Such higher amounts of Cr dissolved in the eta carbide may also contribute in decreasing the amount of Cr carbide dissolved – in experimental samples- in the binder phase at low carbon contents.

5. Conclusion

This investigation on hardmetals with Ru-containing binders of different chemistries (Co, Ni, CoNi and CoNiCr) demonstrates that, in all cases, Ru increases the amount of W and Cr that can be introduced in solid solution in the metallic FCC binder phase, thus increasing the degree of alloying in the system. This is true for both low carbon and high carbon alloys, in equilibrium with eta carbides and graphite, respectively. The solubility of W decreases in the sequence Ni > CoNi> Co > CoNiCr. In the case of Ru containing alloys the sequence is the same NiRu> CoNiRu> CoRu>CoNiCrRu but the absolute values are higher than in the Ru-free variants. This applies also for both low carbon and high carbon alloys. Although the lowest W solubility in the series is always found in the CoNiCr(Ru) binders, the total amount of elements – Cr and W- dissolved in the metallic binder (sum of at.%) is the highest in this system, due to the additional Cr (highest amount of elements in solution in the binder).

Using the difference in the lattice parameter as an indirect indication of the carbon window it is evidenced that the carbon window decreases in the sequence Ni > CoNi> Co/CoNiCr (as one might expect from industrial experience). Same lattice parameter measurements would indicate that Ru increases the size of the carbon window for the systems NiRu, CoRu and CoNiRu, as compared to the same alloys without Ru.

When comparing binders of different chemistries using Co as reference, it is obvious that in general the addition of elements with lower carbon affinity than Co (as Ni and Ru) tends to increase the amount of alloying elements that can be dissolved in the metallic binder, and thus broaden the carbon windows. In the case of Ru, as presented in this study, additions of Ru can significantly change the chemical nature of the binder, increasing the solubility of elements like W, Cr, and possibly also of C.

On the other hand, elements with a high carbon affinity (like Cr), tend to decrease the solubility of W in the binder phase, both at low and at high carbon contents. This phenomenon had been previously proved for Ni-based binders, and it is confirmed in this work also for Ru-containing binders. At high carbon contents, Cr-rich carbides precipitate if the Cr concentration in the binder is beyond its solubility limit. However, due to slow kinetics in the nucleation of these carbides, a certain degree of super saturation in Cr can be observed in the high carbon variants.

In terms of WC grain growth, the different growth behaviour in different binder systems is obviously linked with the chemical composition of the respective binder matrix. The strong impact of the carbon content (activity) on the WC grain growth, determines the chemical environment (solubilities of W and Cr) of the growing WC grains. In general, high solubilities of W in the binder phases have a very strong effect on limiting grain growth, which is evidenced by the fine microstructures observed at low carbon contents for all binder chemistries. At high carbon contents, the solubility of W in the binder phases is considerably reduced, and in this case the presence of additional Cr

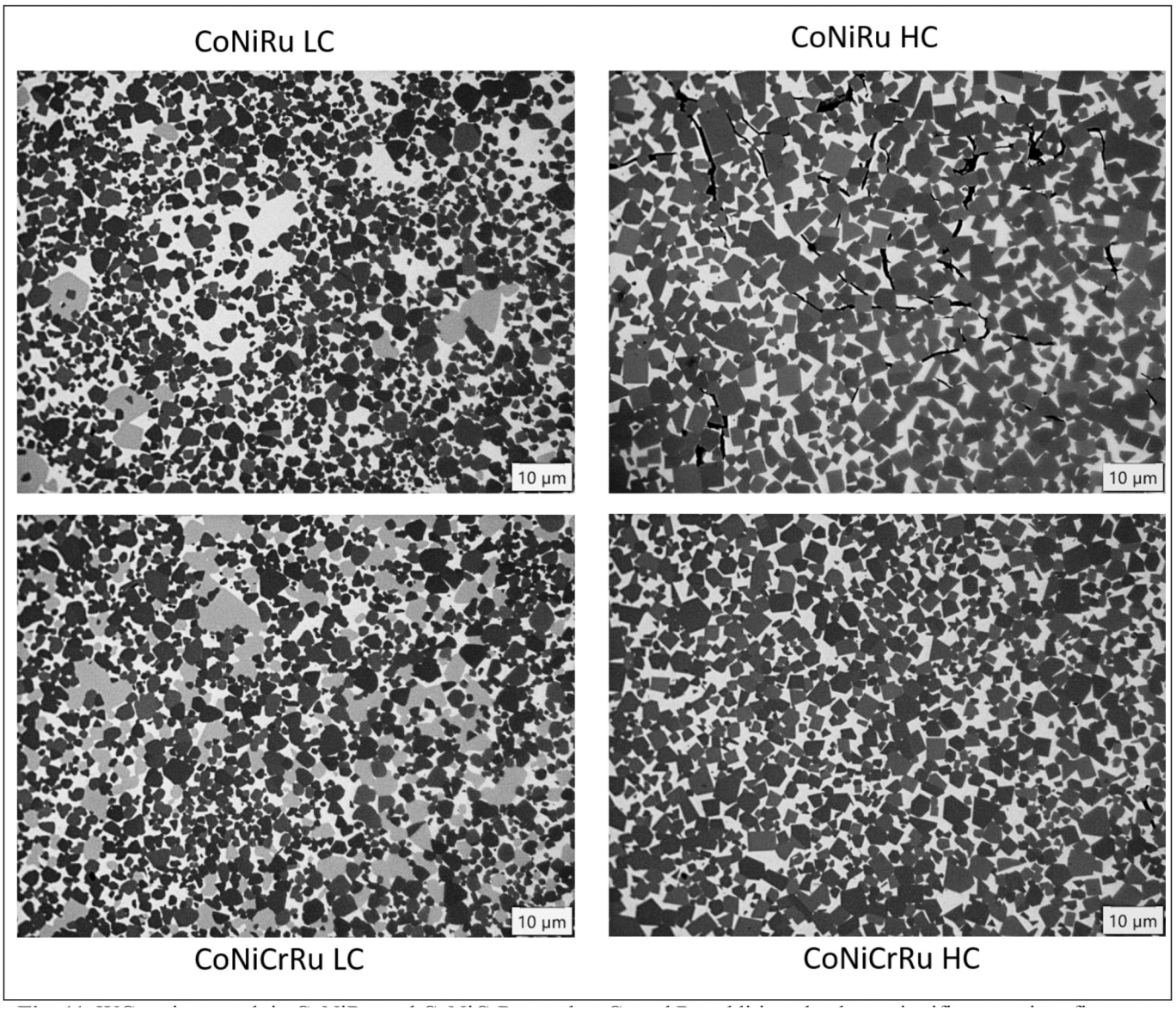

Fig. 11. WC grain growth in CoNiRu and CoNiCrRu grades. Cr and Ru additions lead to a significant grain refinement in both LC and HC alloys.

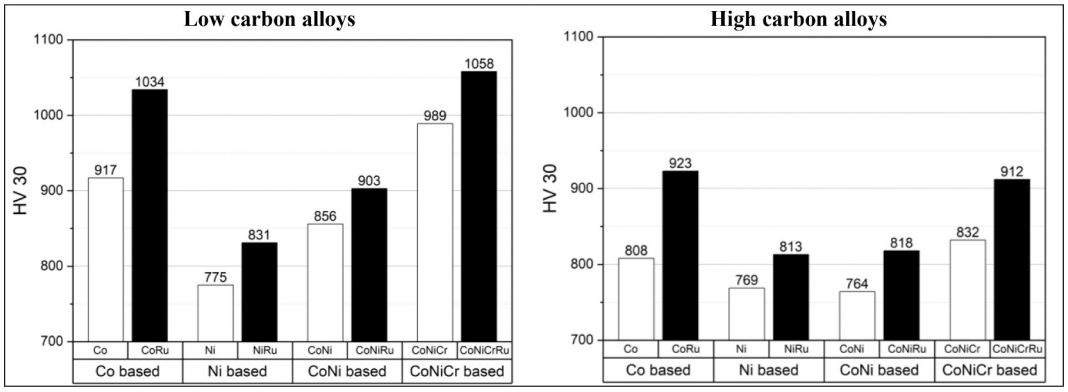

Fig. 12. HV 30 values for all alloys, comparison of each low and high carbon sample and between the Ru-free and Ru containing sample of each system.

seems to play the major role in controlling the grain growth. Ru affects the grain growth in all systems by affecting the chemical nature of the binder (e.g. by increasing the W solubility in the binder).

The higher solubility of W can significantly affect properties like hardness (both due to grain refinement and to solid solution hardening of the binder) and corrosion resistance. This study has set the basis of the

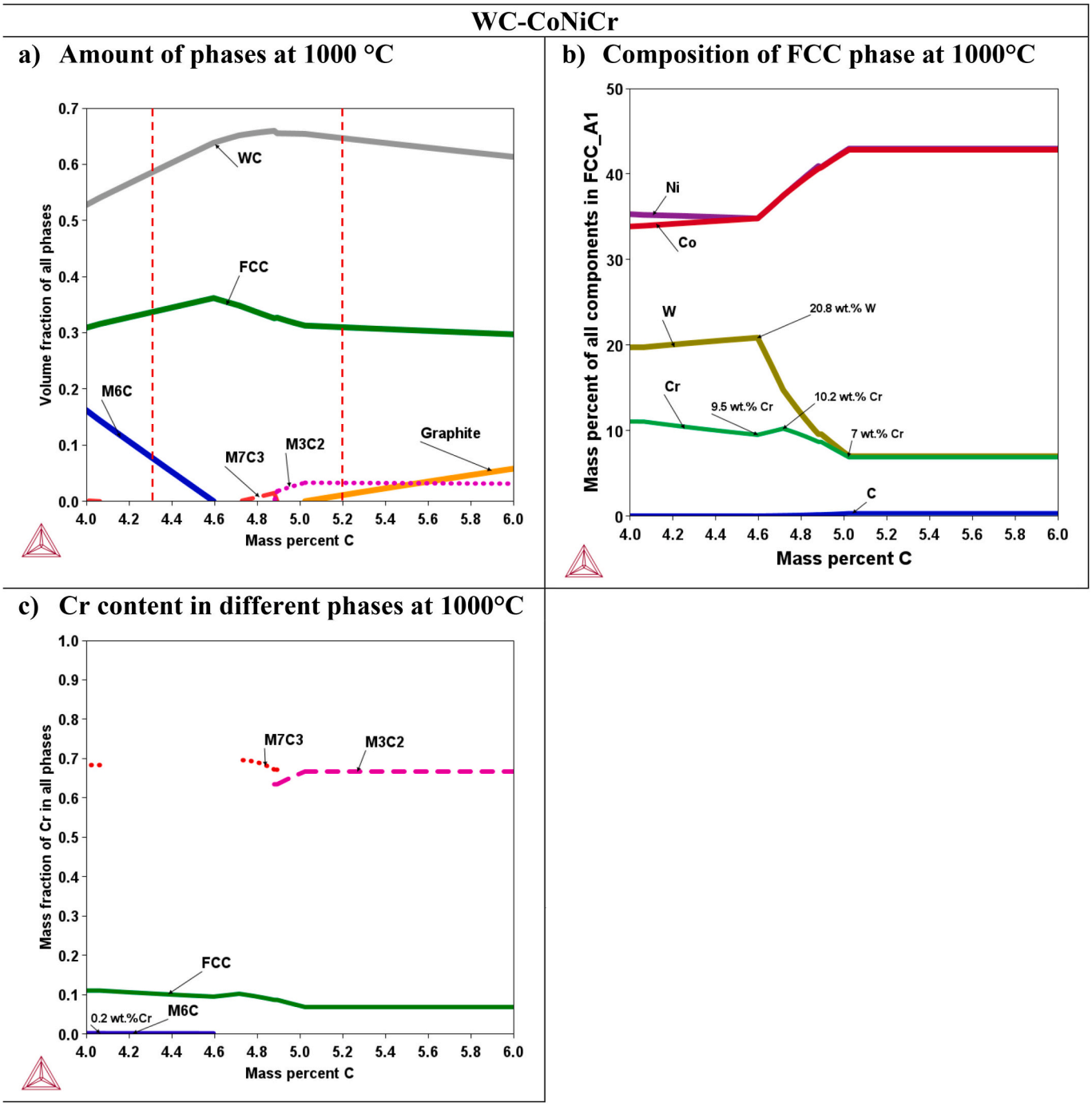

Fig. 13. Thermodynamic calculations at 1000 °C in the system WC-20 wt%(CoNi12wt%Cr), as a function of the carbon content: a) amount of phases stable at 1000 °C, b) composition of the FCC phase at 1000 °C, c) amount of Cr in the different phases at 1000 °C. Calculations were made with the software ThermoCalc using the database TCFE 9.

solubility trends that will be used for selecting samples for high temperature investigations on binders with different chemistries.

CRediT authorship contribution statement

Lena Maria Dorner: Writing – review & editing, Visualization, Validation, Investigation, Funding acquisition, Data curation. **Raquel De Oro Calderon:** Writing – review & editing, Writing – original draft, Visualization, Validation, Supervision, Methodology, Funding acquisition, Formal analysis, Conceptualization. **Wolf-Dieter Schubert:** Writing – review & editing, Writing – original draft, Visualization, Validation, Methodology, Formal analysis, Conceptualization. **Ralph Useldinger:** Writing – review & editing, Validation, Supervision, Resources, Methodology, Funding acquisition, Formal analysis, Conceptualization.

Declaration of competing interest

The authors declare that they have no known competing financial interests or personal relationships that could have appeared to influence the work reported in this paper.

Acknowledgements

The authors would like to acknowledge the financial support by the Luxembourg National Research Fund (FNR) through the project INNOVATE 18180714.

Data availability

Data will be made available on request.

References

[1] J.-W. Yeh, S.-K. Chen, S.-J. Lin, et al., Nanostructured high-entropy alloys with multiple principal elements: novel alloy design concepts and outcomes, Adv. Eng. Mater. 6 (5) (2004) 299–303, https://doi.org/10.1002/adem.200300567.
[2] B. Cantor, et al., Mater. Sci. Eng. A 375-377 (2004) 213–218, https://doi.org/10.1016/j.msea.2003.10.257.
[3] J.-W. Yeh, JOM 65 (12) (2013) 1759–1771, https://doi.org/10.1007/s11837-013-0761-6.
[4] J.-W. Yeh, Ann. Chim. Sci. Mater. 31 (6) (2006) 633–648, https://doi.org/10.3166/acsm.31.633-648.
[5] D.B. Miracle, O.N. Senkov, Acta Mater. 122 (2017) 448–511, https://doi.org/10.1016/j.actamat.2016.08.081.
[6] E.P. George, D. Raabe, R.O. Ritchie, Nat. Rev. Mater. 4 (8) (2019) 515–534, https://doi.org/10.1038/s41578-019-0121-4.
[7] J. Sun, et al., Crit. Rev. Solid State Mater. Sci. 44 (3) (2019) 211–238.
[8] P.K. Katiyar, et al., Adv. Mater. Process. Technol. (2022) 1–38.
[9] B. Straumal, I., Konyashin WC-based cemented carbides with high entropy alloyed binders: a review, Metals 13 (2023), https://doi.org/10.3390/met13010171.
[10] Raquel de Oro Calderon, et al., Novel binders for WC-based cemented carbides with high Cr contents, Int. J. Refract. Met. Hard Mater. 85 (2019) 105063, https://doi.org/10.1016/j.ijrmhm.2019.105063.
[11] H.G. Schmid, D. Mari, W. Benoit, V. Bonjour, The mechanical behaviour of cemented carbides at high temperatures, Mater. Sci. Eng. A 106 (1–2) (1988) 343–351.
[12] T.L. Shing, S. Luyckx, I.T. Northrop, I. Wolff, The effect of ruthenium additions on the hardness, toughness ana grain size of WC-Co, Int. J. Refract. Met. Hard Mater. 19 (2001) 41–44.
[13] L. Chipise, P.K. Jain, L.A. Cornish, Sliding wear characteristics of WC-VC-Co alloys with various Ru additions, Int. J. Refract. Met. Hard Mater. 95 (2021) 105429.
[14] H. Zhang, J. Xiong, Z. Guo, T. Yang, J. Liu, T. Hua, Microstructure, mechanical properties, and cutting performances of WC-Co cemented carbides with Ru additions, Ceram. Int. 47 (2021) 26050–26062.
[15] P. Mehrota, P. Trivedi, G. Roder, Recent advances in ruthenium containing hardmetals, in: World PM2016 – HM Processing II, 2016, pp. 1–6.
[16] Luyckx, High temperature hardness of WC-Co-Ru, J. Mater. Sci. Lett. 21 (2002) 1681–1682.
[17] X. Yang, Q. Tang, X. Zhang, J. Shu, J. Liao, Effect of ruthenium on microstructure and properties of WC-(W, Ti, Ta)C-Co cemented carbide, Mater. Sci. Forum 8993 (2019) 851–856.
[18] A.F. Lisovskii, Cemented carbides alloyed with ruthenium, osmium, and rhenium, Powder Metall. Met. Ceram. 39 (9–10) (2000) 428–433.
[19] S. Olovsjö, J. Qvick, Influence of carbon content on the binder microstructure in WC-Co-Ru cemented carbides, in: 20th International Plansee Seminar, HM 116/1-7, 2022.
[20] W.D. Schubert, R. Steinlechner, R. de Oro Calderon, On the constitution and cobalt alloy formation in WC-1.4 wt% Ru-9.5 wt%Co cemented carbides, Int. J. Refract. Met. Hard Mater. 116 (2023) 106346, https://doi.org/10.1016/j.ijrmhm.2023.106346.
[21] R. Steinlechner, R. de Oro Calderon, T. Koch, P. Linhardt, W.D. Schubert, A study on WC-Ni cemented carbides: constitution, alloy compositions and properties, including corrosion behaviour, Int. J. Refract. Met. Hard Mater. 103 (2022) 105750, https://doi.org/10.1016/j.ijrmhm.2021.105750.
[22] Mehdi Eizadjou, et al., An observation of the binder microstructure in WC-(Co+Ru) cemented carbides using transmission Kikuchi diffraction, Scr. Mater. 183 (2020) 55–60, https://doi.org/10.1016/j.scriptamat.2020.03.010.
[23] Ehsan Farabi, et al., On the fcc to hcp transformation in a Co-Ru alloy: variant selection and intervariant boundary character, Scr. Mater. (2024), https://doi.org/10.1016/j.scriptamat.2024.116127.
[24] Bartek Kaplan, et al., Thermodynamic calculations and experimental verification in the WC-Co-Cr cemented carbide system, Int. J. Refract. Met. Hard Mater. 48 (2015) 257–262, https://doi.org/10.1016/j.ijrmhm.2014.09.016.
[25] Z. Tükör, W.D. Schubert, A. Bicherl, A. Bock, B. Zeiler, Formation of W–Cr–phases during the production of Cr-doped WC powders, in: Proceedings of the 17th Plansee Seminar vol. 4, 2009, pp. 1–10.
[26] A. Delanoë, M. Bacia, E. Pauty, S. Lay, C. Allibert, Cr-rich layer at the WC/Co interface in Cr-doped WC–Co cermets: segregation or metastable carbide? J. Cryst. Growth 270 (2004) 219–227, https://doi.org/10.1016/j.jcrysgro.2004.05.101.
[27] M. Yousfi, A. Nordgren, S. Norgren, J. Weidow, H. Andrén, L. Falk, Creep of un-doped and Cr-doped WC-co at high temperature and high load, Int. J. Refract. Met. Hard Mater. 116 (2023) 106417, https://doi.org/10.1016/j.ijrmhm.2023.106417.
[28] P.K. Mehrotra, P.B. Trivedi, Effect of Binder Composition on Cemented Carbides, Powdermet 2015, 2015 International Conference on Powder Metallurgy & Particulate Materials, MPIF, San Diego, 2015.
[29] Bernhard Wittmann, et al., WC grain growth and grain growth inhibition in nickel and iron binder hardmetals, Int. J. Refract. Met. Hard Mater. 20 (2002) 51–60, https://doi.org/10.1016/S0263-4368(01)00070-1.
[30] Zoé Roulon, et al., Carbide grain growth in cemented carbides sintered with alternative binders, Int. J. Refract. Met. Hard Mater. 86 (2020) 105088, https://doi.org/10.1016/j.ijrmhm.2019.105088.
[31] P.B. Trivedi, P.K. Mehrotra, US Patent 9,725,794 B2 (2017); US Patent 10,415,119 B2, 2019.